Available online at www.sciencedirect.com
ScienceDirect
Journal of Power Sources 167 (2007) 84–89
JOURNAL OF POWER SOURCES
www.elsevier.com/locate/jpowsour

Short communication

Effect of SDC-impregnated LSM cathodes on the performance of anode-supported YSZ films for SOFCs

Kongfa Chen [a], Zhe Lü [a,*], Na Ai [a], Xiangjun Chen [b], Jinyan Hu [a], Xiqiang Huang [a], Wenhui Su [a,c,d]

[a] *Center for Condensed Matter Science and Technology, Harbin Institute of Technology, Harbin 150001, China*
[b] *Division for Theoretical Physics, Harbin Institute of Technology, Harbin 150001, China*
[c] *Department of Condensed Matter, Jilin University, Changchun 130022, China*
[d] *International Center for Material Physics, Academia, Shenyang 110015, China*

Received 3 November 2006; received in revised form 3 January 2007; accepted 3 January 2007
Available online 12 February 2007

Abstract

$Sm_{0.2}Ce_{0.8}O_{1.9}$ (SDC)-impregnated $La_{0.7}Sr_{0.3}MnO_3$ (LSM) composite cathodes were fabricated on anode-supported yttria-stabilized zirconia (YSZ) thin films. Electrochemical performances of the solid oxide fuel cells (SOFCs) were investigated in the present study. Four single cells, i.e., Cell-1, Cell-2, Cell-3 and Cell-4 were obtained after the fabrication of four different cathodes, i.e., pure LSM and SDC/LSM composites in the weight ratios of 25/75, 36/64 and 42/58, respectively. Impedance spectra under open-circuit conditions showed that the cathode performance was gradually improved with the increasing SDC loading. Similarly, the maximum power densities (MPD) of the four cells were increased with the SDC amount below 700 °C. Whereas, the cell performance of Cell-4 was lower than that of Cell-3 at 800 °C, arising from the increased concentration polarization at high current densities. This was caused by the lowered porosity with the impregnation cycle. This disadvantage could be suppressed by lowering the operating temperature or by increasing the oxygen concentration at the cathode side. The ratio of electrode polarization loss in the total voltage drop versus current density showed that the cell performance was primarily determined by the electrode polarization. The contribution of the ohmic resistance was increased when the operating temperature was lowered. When a 100 ml min^{-1} oxygen flow was introduced to the cathode side, Cell-3 produced MPDs of 1905, 1587 and 1179 mW cm^{-2} at 800, 750 and 700 °C, respectively. The high cell outputs demonstrated the merits of the novel and effective SDC-impregnated LSM cathodes.

Keywords: $La_{0.7}Sr_{0.3}MnO_3$ (LSM); Impregnation; $Sm_{0.2}Ce_{0.8}O_{1.9}$ (SDC); Concentration polarization; Mass transfer process

1. Introduction

The solid oxide fuel cell (SOFC) is considered to be one of the most promising fuel cell systems for generating electricity in an efficient and environmentally friendly way [1]. To lower the cost and make commercial applications viable, it is desirable to lower the operating temperature ~1000 °C to a low-to-intermediate temperature range of 500–800 °C.

To reduce the ohmic loss mainly attributed to the thick electrolyte, numerous efforts have been made in fabricating yttria-stabilized zirconia (YSZ) thin films of a few microns thick (5–30 μm) [2–7]. Significant improvements have been achieved due to the substantially reduced electrolyte ohmic resistance. At the same time, further reductions in the electrolyte film would likely result in reliability problems with electrolyte integrity [8].

Eventually, the high cathode polarization resistance becomes the dominant factor limiting the promotion of cell performance in further reducing the temperature. In practice, strontium doped lanthanum manganite (LSM) has been shown to be one of the best cathodic materials found so far in terms of electrochemical activity, thermal and chemical stability and compatibility with YSZ [1]. However, LSM is limited at reduced temperatures due to its low oxygen ion conductivity and high activation energy for oxygen dissociation [9]. The addition of an electrolyte component to the LSM in the formation of composite cathodes dramatically improves the cathode performance [10,11]. This is due to the extension of the three-phase boundary (TPB) regions

* Corresponding author. Tel.: +86 451 86418420; fax: +86 451 86412828.
E-mail addresses: explorer_081@163.com (K. Chen), lvzhe@hit.edu.cn (Z. Lü).

0378-7753/$ – see front matter © 2007 Elsevier B.V. All rights reserved.
doi:10.1016/j.jpowsour.2007.01.088

from the electrolyte/cathode interface deep into the whole electrode.

It was reported that doped ceria (DCO)/LSM composite cathodes had better electrochemical performance than YSZ/LSM composites and seemed to be particularly attractive for low-to-intermediate temperature SOFC [11]. The high ionic conductivity and high oxygen surface exchange coefficient of DCO are suggested as the two main factors aiding electrode processes [11]. Recently, a novel ion-impregnation method [12–15] has been proposed to fabricate the DCO/LSM composites. It is an effective way to deposit electrocatalytic oxide phase into the porous LSM structure without diminishing the advantages of stability and compatibility of LSM materials with YSZ electrolyte [12]. Furthermore, the electrochemical activity of the DCO-impregnated LSM cathodes for O_2 reduction is largely enhanced, e.g., the electrode polarization resistance (R_E) of the impregnated LSM cathodes has been largely reduced to around 0.20 $\Omega\,cm^2$ at 700 °C [13,14]. These are considerable results for the development of LSM-based cathodes at reduced temperatures.

As a matter of fact, most of the high performance (R_E) was derived from a half-cell using a three-electrode [12,13,15] or a symmetric configuration [14]. Few reports have focused on the application of this cathode in a practical fuel cell. The application could reveal the difference of the cathode operating on the half-cell and single fuel cell and thus present a more direct proof of the utility. In the present study, $Sm_{0.2}Ce_{0.8}O_{1.9}$ (SDC)-impregnated $La_{0.7}Sr_{0.3}MnO_3$ (LSM) cathodes were fabricated onto the anode-supported YSZ films to form several single cells. The effect of SDC loading on the cell performance is presented and discussed.

2. Experimental

YSZ powder (TZ-8Y) was purchased from the Tosoh Corp. NiO was synthesized by the precipitation method [16], using $Ni(NO_3)_2{\cdot}6H_2O$ (Analytical reagent, A.R.) and ammonia (A.R.) as the raw materials. The resultant powder was calcined at 1000 °C for 2 h to form a pure NiO phase. In the green anode powder, NiO, YSZ and flour were mixed in the weight ratio of 5:5:2.2, and ground with a mortar and pestle for 2 h. The compacted anode pellets were calcined at 1000 °C for 2 h. 13-μm-thick dense YSZ thin films were deposited onto the NiO-YSZ substrates by slurry spin coating, as reported previously [17,18]. The anode/YSZ film bi-layers were then co-fired at 1400 °C for 2 h.

$Sm_{0.2}Ce_{0.8}O_{1.9}$ (SDC)-impregnated $La_{0.7}Sr_{0.3}MnO_3$ (LSM) cathodes were fabricated. LSM powder was synthesized by the Pechini method, using $La(NO_3)_3{\cdot}6H_2O$ (A.R.), $Sr(NO_3)_2$ (A.R.), $Mn(NO_3)_2$ (A.R.) and citric acid monohydrate (A.R.) as the raw materials. The resultant powder was calcined at 1000 °C for 2 h. To produce additional porosity, LSM was mixed with activated carbon powder in a weight ratio of 10:1. The cathode powder was then mixed with a binder to form a paste and subsequently coated onto the sintered YSZ films. After sintering at 1100 °C for 3 h, the cathodes were then impregnated by a 3 mol l^{-1} $Sm_{0.2}Ce_{0.8}(NO_3)_x$ solution, and treated at 850 °C for 1 h. The impregnation–calcination process was repeated for different cycles to get SDC/LSM compositions with varied weight ratios. For the purpose of comparison, a cell with pure LSM was also fabricated. The cathode layer was about 20 μm thick. The details of the samples are listed in Table 1.

Table 1
Cathode composition of the cells

Sample	Weight ratio of SDC/LSM
Cell-1	0
Cell-2	25:75
Cell-3	36:64
Cell-4	42:58

Fuel cells were tested by the four-probe method, and the schematic of the fuel cell assembly is shown in Fig. 1. Hydrogen was used as fuel and stationary air as oxidant. In some cases, pure oxygen flow was introduced at the cathode side. Electrochemical characteristics were performed with an electrochemical interface SI 1287 and impedance/gain analyzer SI 1260 (Solartron Instruments, Hampshire, UK) from 600 to 800 °C. The impedance spectra were measured in the frequency range from 0.1 Hz to 91 kHz with an AC signal amplitude of 10 mV.

3. Results and discussion

Fig. 2 shows impedance spectra of the four cells under open-circuit conditions at 800 °C. As shown in Table 1, the SDC/LSM weight ratios in the composite cathodes are increasing with the label number. There are two depressed semicircles in every impedance spectroscopy curve, which reflect the electrode polar-

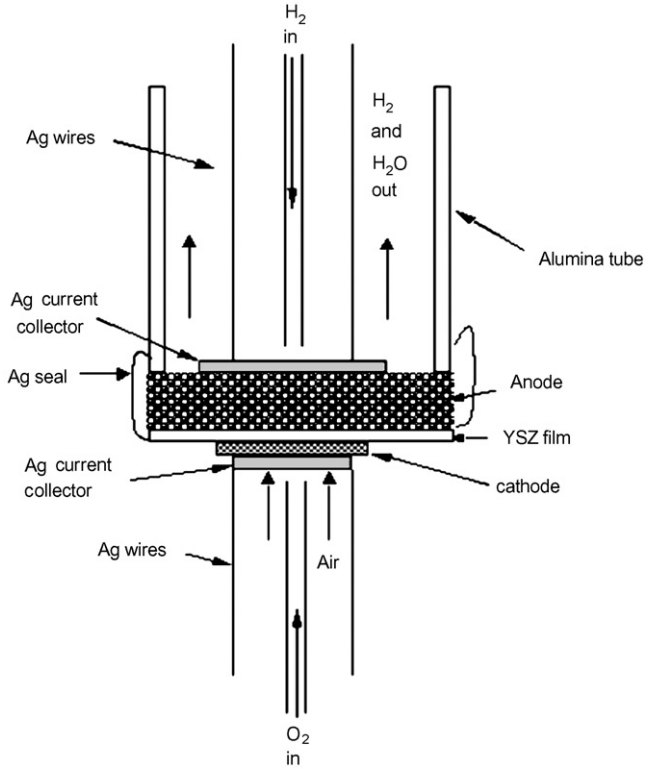

Fig. 1. Schematic of the fuel cell arrangement.

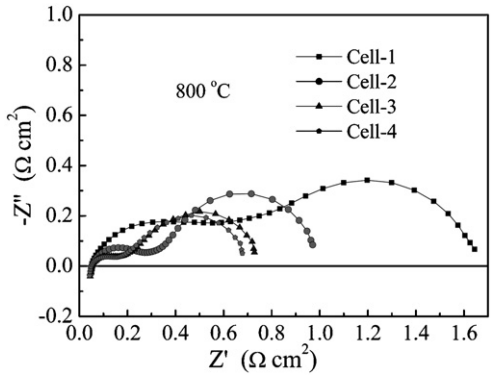

Fig. 2. Impedance spectra of the cells under open-circuit conditions at 800 °C.

ization resistances both from the anode and the cathode. It is known that anode polarization resistance is negligible at low current density compared with that of the cathode [19–21] due to much faster electrochemical oxidation of the hydrogen reaction in the anode. Furthermore, the anode and anode/YSZ bi-layers were fabricated with the same process in the present study. So the difference among the cells should be ascribed to the contribution of the difference in the impregnated cathodes. As can be seen, the curves show similar intercepts at high frequency of the impedance spectra, namely, the ohmic resistance is approximately the same (0.05 Ω cm^2). While the difference between the high and low frequency intercepts, i.e., cathode interfacial resistance is gradually lower with the increase in the SDC ratio. A continuous and porous network of SDC conducting paths was gradually formed with the impregnation cycle. The deposition of nano-sized oxygen conducting phase on the porous LSM surface and at the LSM/YSZ interface region would effectively enhance the TPBs for the O_2 reduction reaction [13]. On the other hand, the existence of the nano-sized SDC particles on the LSM surface could also enhance the oxygen exchange rate [13]. Consequently, the cathode performance is substantially enhanced at low current density. The results are in good accordance with the literatures [12–14].

Fig. 3 presents the electrochemical characteristics of the four single cells at 800 °C. All of the cells produce an open-circuit voltage (OCV) of around 1.10 V, implying that the electrolyte films are crack-free and gas-tight to prevent gas leakage through the cells. Maximum power densities (MPD) are 816, 981, 1322 and 1252 mW cm^{-2} for Cell-1, Cell-2, Cell-3 and Cell-4, respectively. In general, the cell performance is promoted with the increase in SDC loading, which is attributed to the enhanced cathode performance. This is in good agreement with the results in Fig. 2. On the other hand, the MPD of Cell-4 is slightly lower than that of Cell-3. As shown in Fig. 3, the *I–V* characteristics of Cell-3 and Cell-4 nearly superpose at low current densities, and separate apparently when the current density is higher than ~1.75 A cm^{-2}. After that critical point, the voltage of Cell-4 drops more rapidly than that of Cell-3.

It should be noted the porosity of the LSM frame is diminished with the impregnation cycle, since the sequentially added SDC particles would gradually fill up the pores. The ratio of SDC loading in Cell-4 is 6 wt% higher than that in Cell-3. This excessive SDC loading thus further reduce the cathode porosity, posing more limitation on the reactant diffusion rate. When the oxygen consumption rate is much higher than the mass diffusion rate (e.g., when the current density is higher than 1.75 A cm^{-2}), mass transfer process rather than charge transfer process would become the rate-determining step (rds). It thus limits the promotion of the cell performance. This explains the faster voltage drop of Cell-4 due to the higher cathode concentration polarization. As can be expected, mass transfer process could be improved by increasing oxygen gas concentration or by increasing the gas pressure at the cathode side.

Fig. 4 shows the plots of electrode overpotential as a function of current density for the four cells at 800 °C. The overpotentials were obtained through the *I–V* characteristics by subtracting ohmic losses as derived from the impedance spectra (Fig. 2). For the pure LSM cathode in Cell-1, the slope of the curve, i.e., cathode polarization resistance is diminished with the current density, from 1.60 Ω cm^2 at low current density to 0.26, 0.27 and 0.10 Ω cm^2 at 1.0, 2.0 and 3.0 A cm^{-2}, respectively. It should be due to the extension of TPB from the LSM/YSZ interface to the LSM surface as a result of the formation and propagation of oxygen ion vacancies when LSM is under sufficient cathodic polarization [22,23]. This phenomenon can be called as cathode self-promotion process and should be beneficial to the improvement of the cathode performance at a higher current density. However, as can be observed, the self-promotion process in the impregnated LSM cathodes is gradually suppressed, since concentration polarization becomes the dominant factor with the increase of SDC ratio in cathodes. In addition, the ionic con-

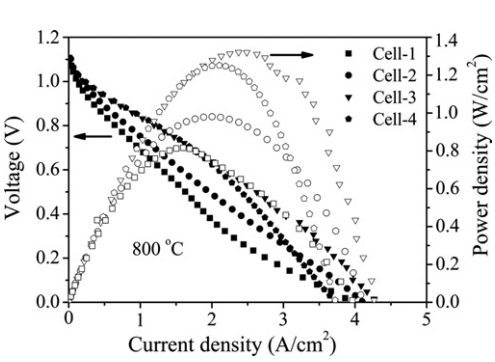

Fig. 3. Electrochemical characteristics of the cells at 800 °C.

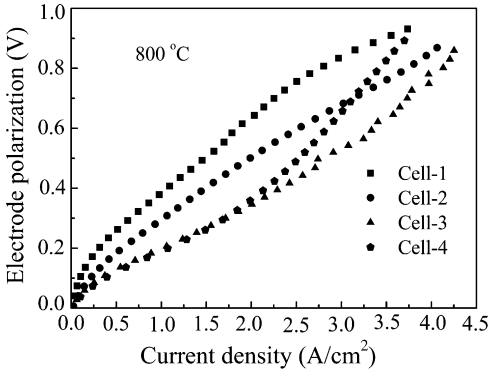

Fig. 4. Electrode polarization vs. current density at 800 °C.

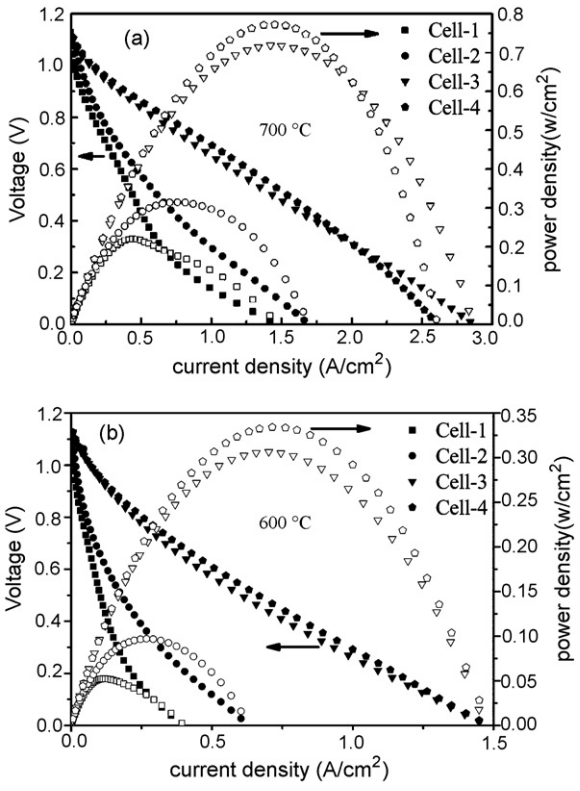

Fig. 5. Electrochemical characteristics of the cells (a) at 700 °C and (b) at 600 °C.

ductivity of the continuous SDC phase should be much higher than that of the self-formed ionic conducting path in the pure LSM. It could also weaken the effect of the self-promotion on the cell performance. Anyhow, the cathode performance at relatively low current density is substantially enhanced with the addition of SDC loading.

Fig. 5a and b shows the *I–V* and *I–P* characteristics of the four cells at 700 and 600 °C, respectively. The MPDs are 220, 315, 719 and 773 mW cm^{-2} at 700 °C and 52, 97, 307 and 334 mW cm^{-2} at 600 °C for the cells from Cell-1 to Cell-4, respectively. Obviously, the cell performance is more dependent on the amount of SDC in the cathode at reduced temperatures than that at elevated temperatures. From this viewpoint, the effectiveness of the impregnated cathode can be readily observed. The concentration polarization limiting the cell performance at 800 °C seems no longer dominant at lower temperatures, due to relatively low short-circuit current densities. Conversely, the charge transfer process becomes the determining factor. As mentioned above, the TPB length is largely enlarged due to the increase of the SDC amount in the LSM structures. Also, the oxygen exchange rate is enhanced by the nano-sized SDC particles. This results in an ever-improved charge transfer process (rds) and a promoted cell performance. As a consequence, the disadvantageous effect of the low porosity has been effectively restricted through the reduction in the operating temperature. The output performance of Cell-4 at the reduced temperature is higher than that of the cell based on YSZ thin film with LSM-YSZ composite cathode [5,6,24], LSCF cathode [6,25] and YSB-Ag cathode [26], implying the advantage of the impregnation cathodes in the development of low-to-intermediate temperature SOFC. Also the impregnation process opens an effective route for easily controlling the cell performance at different operating temperature. For example, when a relatively high performance is required at intermediate temperature around 800 °C, the content of SDC in the composite cathode should be controlled less than 36 wt%. On the contrary, the amount should be increased to more than 42 wt% when a desirable output performance is needed at lower temperatures below 700 °C. The details concerning a threshold ratio on the cell performance at various temperature ranges should be worked out in the future.

The ratio of electrode polarization loss (η) in the overall cell voltage drop ($\eta + iR_{ohm}$) is quite different at various current densities, and the relations at 800, 700 and 600 °C are plotted in Fig. 6. In general, the ratio becomes gradually lower with the increase in the SDC content. Exceptionally, the value of Cell-4 keeps rising after reaching a peak at 800 °C, which

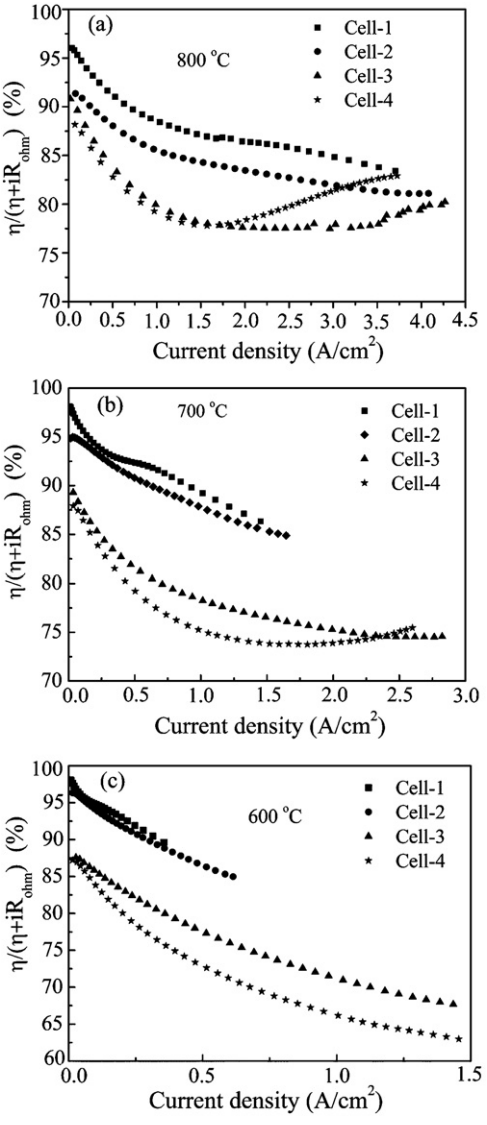

Fig. 6. The ratio of electrode polarization loss in the total cell voltage loss versus current at (a) 800 °C, (b) 700 °C and (c) 600 °C, respectively.

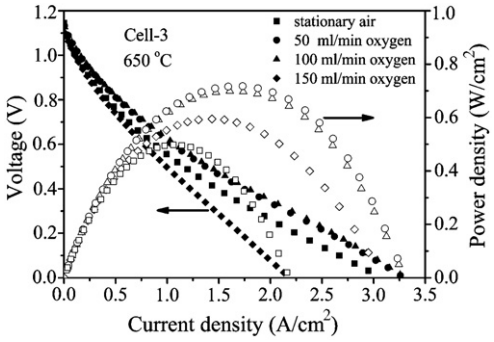

Fig. 7. The effect of oxygen flow rate on the cell performance of Cell-3.

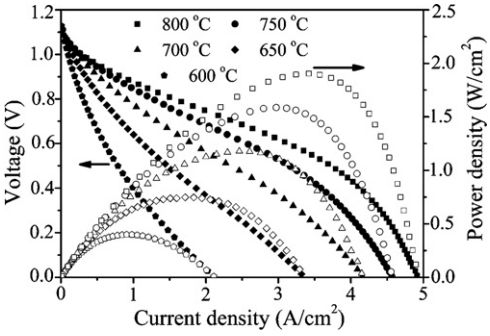

Fig. 8. Electrochemical characteristics of Cell-3 when 100 ml min^{-1} oxygen was introduced.

is relevant to the shift of the rds from charge transfer process to mass transfer process. This phenomenon is gradually suppressed with the decreasing temperature and the effectiveness of the impregnated LSM cathodes with a high SDC content is clear at 600 °C. This corresponds with the *I–V* and *I–P* characteristics at reduced temperatures. Furthermore, note that the ohmic polarization loss around the very current density at MPD accounts for not a small part as it does in the low current density region. For a single cell with the high performance cathode, the contributions of the electrode polarization and ohmic polarization are almost identical at low temperature (see Fig. 6c). So reduction of the YSZ film thickness from 13 μm in the present study to 5 μm would lead to a considerable increase in the cell performance. On the other hand, other ZrO_2-based electrolytes with higher oxygen ionic conductivities would be the alternative candidates to lower the electrolyte ohmic resistance, e.g., $(CeO_2)_{0.01}$–$(Sc_2O_3)_{0.10}$–$(ZrO_2)_{0.89}$ (1Ce10ScZr) [4], $(Sc_2O_3)_{0.10}$–$(Y_2O_3)_{0.01}$–$(ZrO_2)_{0.89}$ (SYSZ) [27].

Shown in Fig. 7 are the electrochemical characteristics of Cell-3 with the cathode exposed to different gas conditions. The MPD of the cell is 498 mW cm^{-2} with the cathode exposed to stationary air. It increases to 599, 699 and 718 mW cm^{-2} when 50, 100 and 150 ml min^{-1} oxygen flows are introduced, respectively. Obviously, compared with the result using air as the oxidant, the performance is largely promoted by the oxygen flow, e.g., it is increased by 44% when 150 ml min^{-1} oxygen flow is introduced. The OCV is affected by the oxygen flow, e.g., the OCV changes from 1.12 to 1.14 V when the oxidant is changed from the air to 50 ml min^{-1} oxygen. This, to some extent, would be beneficial to enhance the cell performance. Introduction of the oxygen in the cathode increases the oxygen concentration and oxygen partial pressure (corresponded to the increased OCV) and boosts the oxygen transport rate at the cathode layer, which is an effective means to improve the mass transfer process. Meanwhile, the added oxygen flow would also lead to improved charge transfer process by supplying sufficient reactant to the TPB sites. In a word, the introduced oxygen flow leads to promoted cathode performance, including the mass and charge transfer processes. It should be noted that the cell shows similar performance with 100 and 150 ml min^{-1} oxygen flows. Any further increase in the oxygen flow would be of negligible help. Since the gas-phase diffusion is sufficient at relatively low temperature, charge transfer process, typically dissociative adsorption of oxygen on the electrode surface, turns to be the rds. Therefore, 100 ml min^{-1} oxygen flow is chosen to introduce at the cathode side at other temperatures.

Fig. 8 presents the electrochemical characteristics of the Cell-3 with 100 ml min^{-1} oxygen oxidant. The MPDs are 1905, 1587, 1179, 748 and 400 mW cm^{-2} at 800, 750, 700, 650 and 600 °C, respectively. With the enhancement in the cathode performance, a considerable improvement of the cell performance at low-to-intermediate temperature is successfully achieved. Comparison of the cell performance with the cathode under air and oxygen conditions is complied in Table 2. Compared with the air oxidant, the contribution of oxygen flow on the cell performance is increased with temperature lower than 700 °C. After that, the promotion in the cell performance is decreased with the temperature. This can be regarded as a shift of the rds from one step to another at the critical point of 700 °C, namely, from a charge transfer process to a mass transfer process, which is the primary factor limiting further promotion of cell performance. On the other hand, the cell performance above 700 °C could be further improved when oxygen with much higher flow rate was provided.

It should be noted that the cell performance with the SDC-impregnated LSM cathodes at low temperature is ever increased along with the optimization of the impregnation fabrication process in our studies, e.g., MPDs at 650 °C are 420 mW cm^{-2} in literature [17], 493 mW cm^{-2} in literature [18] and 545 mW cm^{-2} derived from Cell-4 in this study. As can be expected, further optimization of the cathode fabrication process, including the LSM fabrication process and the solution impregnation process, should result in a substantial decrease in the cathode polarization loss. Meanwhile, use of this high perfor-

Table 2
Cell performance of Cell-3 when the cathode was exposed to varied atmospheres

Temperature (°C)	MPD in air p (mW cm^{-2})	MPD in oxygen p' (mW cm^{-2})	$(p'-p)/p$ (%)
800	1322	1905	44
750	1010	1587	57
700	719	1179	64
650	498	748	50
600	307	400	30

mance cathode opens an effective route to feasible commercial realization of low-to-intermediate temperature SOFCs based on the standard YSZ electrolyte. At the same time, it should be noted that the anode would pose a limitation on further promotion of the cell performance. It is known that anode polarization resistance is almost negligible at low current density. However, it becomes comparable with the cathode polarization resistance at relatively high current densities [20,28]. Using another anode substrate by Wang et al. [29], a single cell with the similar SDC-impregnated cathodes yielded high MPDs of 2005 and 1567 mW cm^{-2} at 800 and 750 °C, respectively. This means that there is still large room for cell performance improvement based on this effective cathode.

4. Conclusion

Anode-supported YSZ thin films with SDC-impregnated LSM cathodes were fabricated. The electrochemical reduction reaction rate of the LSM cathodes was significantly enhanced by the impregnated-SDC particles. Impedance spectra under open-circuit conditions showed that the cathode performance was gradually improved with increasing loading in SDC. However, the cathode with a higher SDC content resulted in a lower electrode porosity. Mass transfer processes therefore became the primary factor in limiting further promotion of cell performance at high current density. This, to some extent, could be settled by lowering the operating temperature or by increasing the oxygen concentration. An optimized performance would be obtained when a threshold relevant to a reasonable porosity and a sufficient three-phase boundary was achieved. Meanwhile, a novel and effective method was also proposed concerning controlling cell performance at varied temperatures by changing the content of SDC in the LSM structures. A better cell performance was expected to be achieved through further optimization of the LSM microstructure, the solution impregnation process and by choosing a high performance anode substrate.

Acknowledgement

The authors gratefully acknowledge the financial supports from the Ministry of Science and Technology of China under contract no. 2001AA323090.

References

[1] Y. Jiang, S.Z. Wang, Y.H. Zhang, J.W. Yan, W.Z. Li, Solid State Ionics 110 (1998) 111–119.
[2] J.M. Wang, Z. Lü, X.Q. Huang, K.F. Chen, N. Ai, J.Y. Hu, W.H. Su, J. Power Sources 163 (2007) 957–959.
[3] Y.H. Zhang, X.Q. Huang, Z. Lu, Z.G. Liu, X.D. Ge, J.H. Xu, X.S. Xin, X.Q. Sha, W.H. Su, J. Power Sources 160 (2006) 1065–1073.
[4] Z.W. Wang, M.J. Cheng, Y.L. Dong, M. Zhang, H.M. Zhang, J. Power Sources 156 (2006) 306–310.
[5] X.S. Xin, Z. Lü, X.Q. Huang, X.Q. Sha, Y.H. Zhang, W.H. Su, J. Power Sources 159 (2006) 1158–1161.
[6] J. Liu, S.A. Barnett, J. Am. Ceram. Soc. 85 (2002) 3096–3098.
[7] W.T. Bao, Q.B. Chang, R.Q. Yan, G.Y. Meng, J. Membr. Sci. 252 (2005) 175–181.
[8] R. Doshi, V.L. Richards, J.D. Carter, X.P. Wang, M. Krumpelt, J. Electrochem. Soc. 146 (1999) 1273–1278.
[9] X.Y. Xu, C.R. Xia, G.L. Xiao, D.K. Peng, Solid State Ionics 176 (2005) 1513–1520.
[10] T. Tsai, S.A. Barnett, Solid State Ionics 93 (1997) 207–217.
[11] E. Perry Murray, S.A. Barnett, Solid State Ionics 143 (2001) 265–273.
[12] S.P. Jiang, Y.J. Leng, S.H. Chan, K.A. Khor, Electrochem. Solid-State Lett. 6 (2003) A67–A70.
[13] S.P. Jiang, W. Wang, Solid State Ionics 176 (2005) 1351–1357.
[14] S.P. Yoon, J. Han, S.W. Nam, T.-H. Lim, I.H. Oh, S.-A. Hong, Y.-S. Yoo, H.C. Lim, J. Power Sources 106 (2002) 160–166.
[15] X.Y. Xu, Z.Y. Jiang, X. Fan, C.R. Xia, Solid State Ionics 177 (2006) 2113–2117.
[16] K.F. Chen, Z. Lü, X.J. Chen, N. Ai, X.Q. Huang, B. Wei, J.Y. Hu, W.H. Su, J. Alloys Compd. (2007), doi:10.1016/j.jallcom.2006.12.130.
[17] K.F. Chen, Z. Lü, N. Ai, X.Q. Huang, Y.H. Zhang, X.S. Xin, R.B. Zhu, W.H. Su, J. Power Sources 160 (2006) 436–438.
[18] K.F. Chen, Z. Lü, N. Ai, X.Q. Huang, Y.H. Zhang, X.D. Ge, X.S. Xin, X.J. Chen, W.H. Su, Solid State Ionics 177 (2007) 3455–3460.
[19] N.Q. Minh, J. Am. Ceram. Soc. 76 (1993) 563–588.
[20] S. de Souza, S.J. Visco, L.C. De Jonghe, Solid State Ionics 98 (1997) 57–61.
[21] T. Tsai, S.A. Barnett, Solid State Ionics 93 (1997) 207–217.
[22] Y. Jiang, S. Wang, Y. Zhang, J. Yan, W. Li, J. Electrochem. Soc. 145 (1998) 373.
[23] E. Maguire, B. Gharbage, F.M.B. Marques, J.A. Labrincha, Solid State Ionics 127 (2000) 329–335.
[24] L. Besra, C. Compson, M.L. Liu, J. Am. Ceram. Soc. 89 (2006) 3003–3009.
[25] P.V. Dollen, S. Barnett, J. Am. Ceram. Soc. 88 (2005) 3361–3368.
[26] X.Y. Xu, C.R. Xia, S.G. Huang, D.K. Peng, Ceram. Int. 31 (2005) 1061–1064.
[27] K. Yamahara, C.P. Jacobson, S.J. Visco, X.-F. Zhang, L.C. De Jonghe, Solid State Ionics 176 (2005) 275–279.
[28] Y. Jiang, A.V. Virkar, F. Zhao, J. Electrochem. Soc. 148 (2001) A1091–A1099.
[29] J.M. Wang, Z. Lü, K.F. Chen, X.Q. Huang, N. Ai, J.Y. Hu, Y.H. Zhang, W.H. Su, J. Power Sources 164 (2007) 17–23.